

# Engineering Notes

ENGINEERING NOTES are short manuscripts describing new developments or important results of a preliminary nature. These Notes should not exceed 2500 words (where a figure or table counts as 200 words). Following informal review by the Editors, they may be published within a few months of the date of receipt. Style requirements are the same as for regular contributions (see inside back cover).

## Unsteady Rolling Moment Characteristics for Fighter Oscillating with Yawing–Rolling Coupled Motion

Da Huang and Genxing Wu

Nanjing University of Aeronautics and Astronautics, 210016  
Nanjing, People's Republic of China

DOI: 10.2514/1.21144

### Nomenclature

$f$	=	oscillation frequency
$m_x$	=	rolling-moment coefficient in the body axis
$t$	=	time
$\alpha$	=	angle of attack
$\beta$	=	angle of sideslip
$\theta, \psi, \phi$	=	Euler angles
$\theta'$	=	pitch angle
$\psi'$	=	yaw angle
$\phi'$	=	roll angle
$\omega$	=	angular velocity

### Subscripts

$m$	=	amplitude of oscillation angles
$x, y$	=	body coordinates

### Introduction

THE maneuvering flight of an aircraft is very complicated. It usually consists of coupled motions about three body axes; therefore, it is very important to simulate maneuvering flight and measure the unsteady aerodynamics in the wind tunnel. Simple flight maneuvers such as the cobra maneuver [1] and the wing rock can be simulated easily, and tests have been conducted in many wind tunnels [2,3]. However, for the complicated flight maneuvers, such as the Herbst maneuver [4], there is a yawing–rolling coupled motion about the body axes when the aircraft encounters high angles of attack. Up to now, the wind-tunnel test data for such complicated coupled motions are very few. The method of the linear superposition is usually used to calculate the unsteady forces and moments of coupled motion to analyze the maneuvering characteristics of the aircraft. The linear superposition model is suitable at low angles of attack, but whether it is suitable at high angles of attack is still not clear. In [5], Zhongjun and Edward adopted the quasi-steady aerodynamic model and the unsteady aerodynamic model to simulate the coupled motion of the aircraft. The results of the two methods are very different. In this

investigation, an aircraft configuration with a strake wing was tested in a 3-m low-speed wind tunnel at Nanjing University of Aeronautics and Astronautics (NUAA) with large amplitude oscillation. The unsteadiness of the rolling moment as the model oscillates in a yawing–rolling coupled motion is compared with that of in pure yawing motion and rolling motion. The lateral dynamic derivatives were obtained using a mathematical model with the fuzzy logic algorithm and the dynamic derivative simulation. The unsteady rolling moment for the yawing–rolling coupled motion was obtained by using the quasi-steady aerodynamic model or the unsteady aerodynamic model, respectively, and the results are compared with the experimental data. It is shown that the wind-tunnel tests can provide better results for the unsteady aerodynamics of coupled motion at large angles of attack.

### Model and Wind-Tunnel Test

#### Wind Tunnel

All experimental investigations were carried out in the NH-2 2.5 m high by 3 m wide by 6 m long wind tunnel at NUAA. NH-2 is a closed return circuit low-speed wind tunnel, and the maximum velocity is 90 m/s.

#### Test Model

The test model is an aircraft configuration and is shown in Fig. 1. It has a double ventral intake duct, and it has strake wings and a twin-finned tail. The span of the model is 0.7364 m, the expanding length is 0.5164 m, the wing area is 0.0888 m<sup>2</sup>, and the mean aerodynamic chord is 0.2036 m.

#### Dynamic Experimental Equipment

The experimental equipment consists of the model support, the drive setup of oscillation, the control setup, and the data acquisition and processing system. The model support is shown in Fig. 2. The swing cylinder 1 can be slipped along the immobility support to change the pitch angles of the model and can drive the swing support rotating about the  $O$ – $O$  axes to carry out the yawing of the model. The swing cylinder 6 can drive the support sting rotating about the  $Z$ – $Z$  axes to carry out the rolling of the model. The two swing cylinders can be controlled independently.

The oscillation rules of yawing or rolling for the model are described by

$$\psi' = -\psi_m \cos(2\pi ft) \quad (1)$$

$$\phi' = \phi_m \cos(2\pi ft) \quad (2)$$

where  $\psi_m$  and  $\phi_m$  are the angle amplitudes for the model oscillating in yawing or rolling motion, respectively. As the model oscillates in yawing–rolling coupled motion, the frequencies in Eqs. (1) and (2) are identical.

When the pitch angles of the model are different, the Euler angles of the model are given, respectively, by

$$\theta = \arcsin(\sin \theta' \cos \psi') \quad (3)$$

$$\psi = \arctan(\tan \psi' / \cos \theta') \quad (4)$$

Received 15 November 2005; revision received 30 March 2006; accepted for publication 28 April 2006. Copyright © 2006 by the American Institute of Aeronautics and Astronautics, Inc. All rights reserved. Copies of this paper may be made for personal or internal use, on condition that the copier pay the \$10.00 per-copy fee to the Copyright Clearance Center, Inc., 222 Rosewood Drive, Danvers, MA 01923; include the code \$10.00 in correspondence with the CCC.

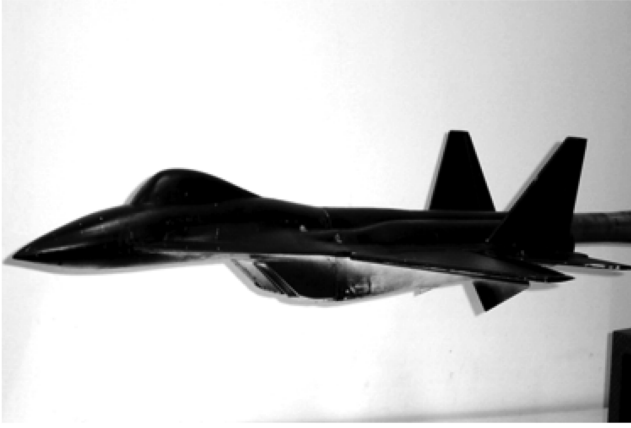
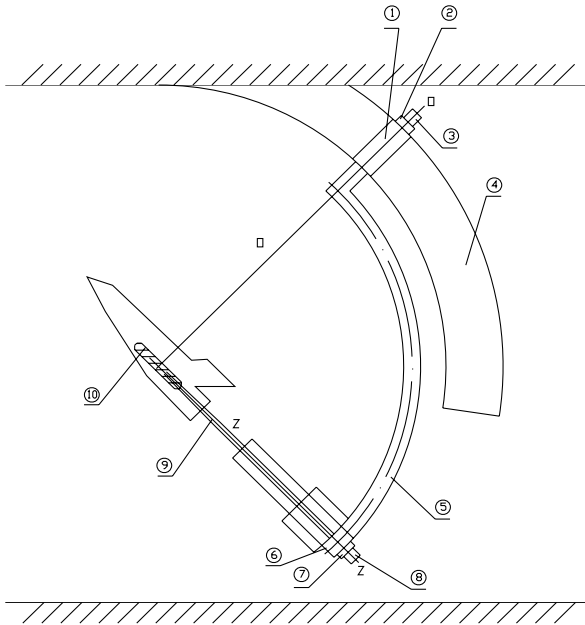


Fig. 1 Photo of the BJ-1 fighter model.



- ①⑥-Swing cylinder ②⑦-Feedback potentiometer  
 ③⑧-Angle coder ④-Fixing support  
 ⑤-Swing support ⑨-Model support sting  
 ⑩-Six component balance

Fig. 2 Sketch of model support.

$$\phi = \phi' \quad (5)$$

The sideslip angle can be obtained from Eq. (6).

$$\sin(\beta) = \sin(\psi) \cos(\phi) + \sin(\phi) \sin(\theta) \cos(\psi) \quad (6)$$

#### Test Result

As the pitch angle of the model was taken at 30 deg, the rolling moments of the model were measured while the model oscillated in yawing, rolling, and yawing–rolling motions independently, and the results are shown in Fig. 3. It is shown that the hysteresis loop of the rolling moment is counterclockwise for all motions and is indicated that the unsteady rolling-moment characteristic for the yawing and rolling motion is consistent with that of for the yawing–rolling motion.

As the pitch angle of the model was taken at 60 deg, the rolling moments of the model were measured while the model oscillated in

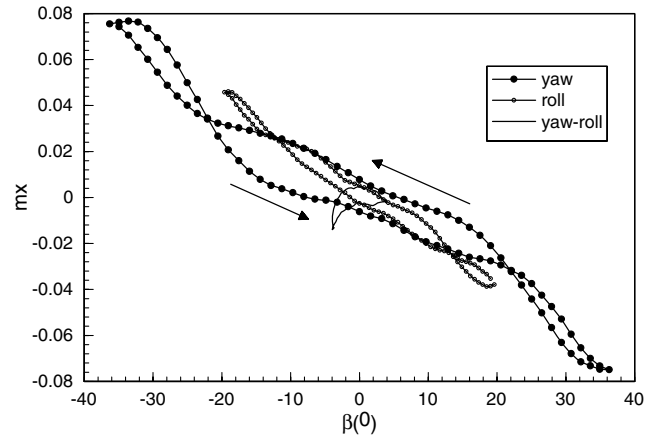


Fig. 3 Unsteady rolling moment at different motions ( $\theta' = 30$  deg).

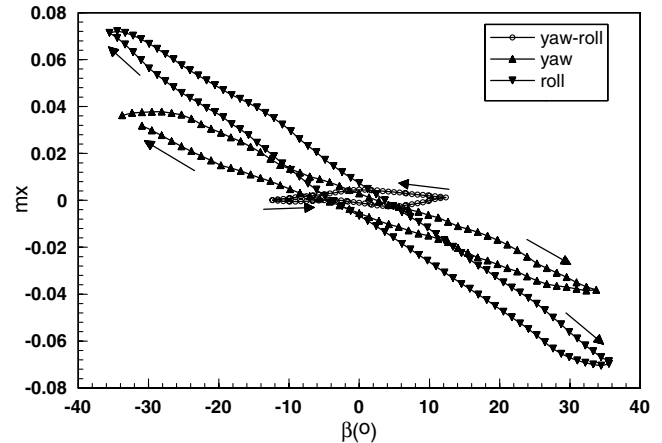


Fig. 4 Unsteady rolling moment at different motions ( $\theta' = 60$  deg).

yawing, rolling, and yawing–rolling motions independently, and the results are shown in Fig. 4. It is shown that the hysteresis loop of the rolling moment for yawing or rolling motions is clockwise. But the hysteresis loop of the rolling moment for yawing–rolling coupled motion is counterclockwise. It is indicated that the unsteady rolling-moment characteristic appears to have a hypostatic difference between pure rolling and coupled motion.

#### Aerodynamic Modeling and Dynamic Derivative Simulation

For the test result of pure motion, the variables of  $\alpha$ ,  $d\alpha/d\beta$ ,  $\beta$ ,  $d\beta/dt$ , and  $f$  were used as the modeling parameters to calculate the mathematical model [6]. The aerodynamic hysteresis loop can be obtained when the model was oscillated with a small amplitude by the mathematical model. On this base, the dynamic derivative and crossed derivative of rolling moment can be computed using the dynamic derivative simulation [7].

The dynamic derivatives obtained from the pure rolling motion are  $m_x^{\omega_x} + m_x^{\dot{\beta}} \sin(\alpha)$  and  $m_x^{\beta} \sin(\alpha) - \omega_x^2 m_x^{\omega_x}$ . The dynamic derivatives obtained from the pure yawing motion are  $m_x^{\omega_y} + m_x^{\dot{\beta}} \cos(\alpha)$  and  $m_x^{\beta} \cos(\alpha) - \omega_y^2 m_x^{\omega_y}$ . As an example, the computed results of several dynamic derivatives at two typical pitch angles are given in Table 1.

In the course of dynamic derivative simulation, the simulation results of dynamic derivatives were significantly affected by the magnitude of the oscillation frequency and the angle amplitude. According to the magnitude of the angular velocity of the yawing and rolling motions while an aircraft was oscillating in a yawing–rolling coupled motion, the dynamic derivatives were calculated. In this paper, the oscillation angle amplitude is 1 deg and the oscillation frequency is 32 Hz.

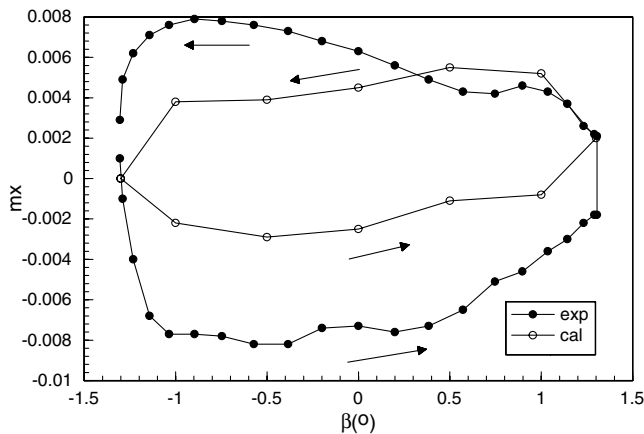
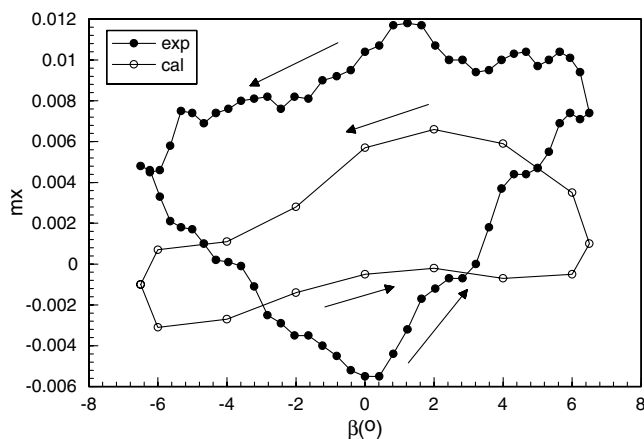
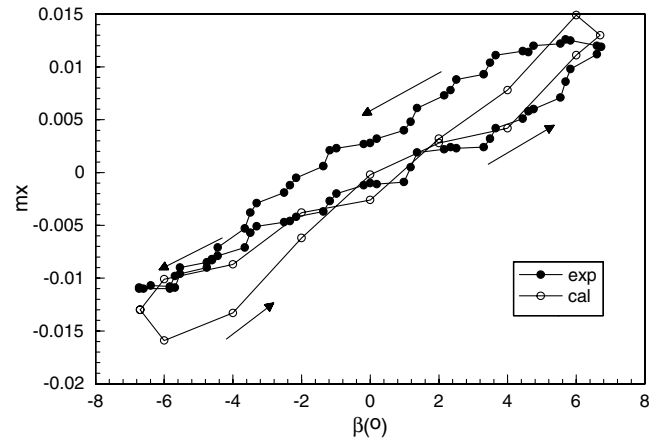
**Table 1 Dynamic derivative at two pitch angles**

$\theta'$	$m_x^{\omega_x} + m_x^{\dot{\beta}} \sin(\alpha)$	$m_x^{\omega_y} + m_x^{\dot{\beta}} \cos(\alpha)$
30 deg	-0.1148	-0.3184
60 deg	0.1865	0.1621

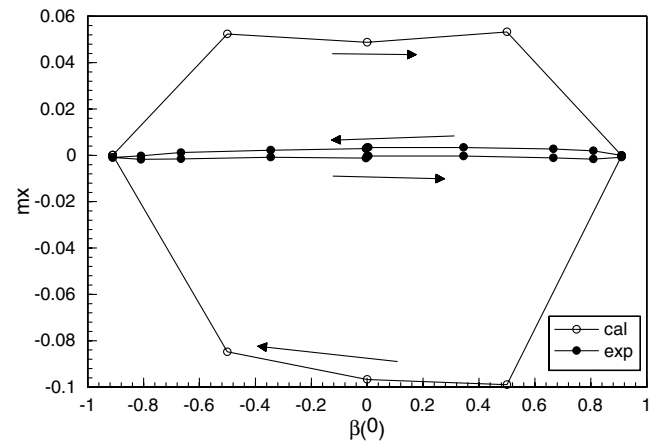
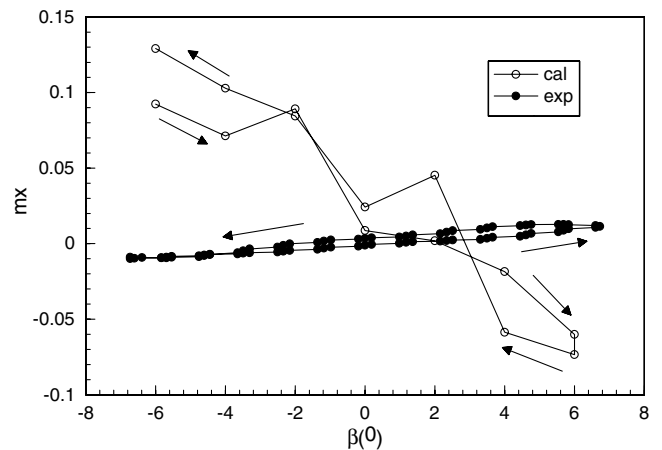
Usually, the small perturbation principle is used to calculate the dynamic characteristics of flight, and the linear superposition principle is adopted to obtain the forces and moments of yawing–rolling coupled motion. When the sideslip angle is in small amplitude, the rolling moment can be described in the following form:

$$m_x = m_{x0} + \left\{ \left[ m_x^{\beta} \sin(\alpha) - \omega_x^2 m_x^{\dot{\omega}_x} \right] + \left[ m_x^{\beta} \cos(\alpha) - \omega_y^2 m_x^{\dot{\omega}_y} \right] \right\} \beta + \left[ m_x^{\omega_x} + m_x^{\dot{\beta}} \sin(\alpha) \right] \omega_x + \left[ m_x^{\omega_y} + m_x^{\dot{\beta}} \cos(\alpha) \right] \omega_y \quad (7)$$

The previous research showed that the term of  $\omega_x^2 m_x^{\dot{\omega}_x}$  and  $\omega_y^2 m_x^{\dot{\omega}_y}$  had a small effect on  $m_x$  and so it can be ignored. The first two terms on the right-hand side of Eq. (7) can be substituted by the static value corresponding to  $\beta$ , and the dynamic derivatives of the third and the fourth terms can be obtained using the dynamic derivative simulation. The two terms of  $\omega_x$  and  $\omega_y$  can be considered the corresponding angular velocity in the yawing–rolling coupled motion.

**Fig. 5 Comparison between the quasi-steady superposition result and the test result ( $\theta' = 30$  deg).****Fig. 6 Comparison between the quasi-steady superposition result and the test result ( $\theta' = 45$  deg).****Fig. 7 Comparison between the quasi-steady superposition result and the test result ( $\theta' = 60$  deg).**

Figures 5–7 display the comparison between the result from superposition theory and the test result with the model in yawing–rolling coupled motion at different pitch angles. From Figs. 5 and 6, the superposition result and the test result are accordant for the quantity. For the movement direction of the hysteresis loop, both directions are accordant while the angle of attack is less than 45 deg. For example, when  $\theta'$  in Fig. 6 is 45 deg, the hysteresis loop of the rolling moment of the superposition result and the test result are counterclockwise. It shows that the single free aerodynamic

**Fig. 8 Comparison between the unsteady superposition result and the test result ( $\theta' = 30$  deg).****Fig. 9 Comparison between the unsteady superposition result and the test result ( $\theta' = 60$  deg).**

superposition result at the medium and large angles of attack has accuracy on a certain extent and can reflect the aerodynamic damp characteristic and divergent characteristic.

As showing in Fig. 7, the single free aerodynamic superposition result and the test result have a large deviation on the quantity at very large pitch angles, and the direction of hysteresis loop appears contrary to change. It is shown that the superposition principle cannot reflect the aerodynamic damp characteristic and divergent characteristic at very large pitch angles.

### Unsteady Aerodynamic Superposition

The unsteady aerodynamic superposition model can be described simply in Eq. (8).

$$m_x = m_{x0s} + m_{xr} + m_{xy} \quad (8)$$

where  $m_{x0s}$  can be obtained from the static test as the model was supported at a yawing angle and a rolling angle.  $m_{xr}$  can be obtained from the pure rolling motion test by taking out the static rolling moment from the unsteady rolling moment.  $m_{xy}$  can be obtained from the pure yawing motion test by the same method as above.

When the pitch angle is taken at 30 and 60 deg, the comparison between the unsteady aerodynamic superposition results, and the test results with the model in the yawing–rolling coupled oscillation can be seen in Figs. 8 and 9. It is obvious from the figure that the linear superposition results and the test results have a large difference not only on the quantity but also on the direction of hysteresis loop. It can indicate that the unsteady superposition principle is not suitable anymore at large pitch angles due to the nonlinear behavior of aerodynamic characteristic.

### Conclusions

By the comparison with the results of two linear superposition models and the test results of the model in the yawing–rolling coupled oscillation, it is found that, for the configuration of aircraft

discussed in this paper, the single free aerodynamic quasi-steady linear superposition principle can reflect the unsteady aerodynamic characteristics at medium and large pitch angles, such as 30 deg. However, when the pitch angle is larger than 50 deg, the single free quasi-steady aerodynamic superposition results do not match the test results for the model oscillating in the yawing–rolling coupled motion, and the quasi-steady superposition principle is not valid anymore. The unsteady aerodynamic superposition results cannot reflect the hysteresis characteristics of the yawing–rolling coupled motion even at small pitch angles. It is also shown that for a high maneuvering aircraft, the accurate unsteady aerodynamic results at large angles of attack can be obtained only by the coupled wind-tunnel tests.

### References

- [1] Zbigniew, D., Grzegorz, K., and Krzysztof, S., "Method of Control of a Straked Wing Aircraft for Cobra Maneuvers," International Council of the Aeronautical Sciences, Rept. 96-3.7.4, 1996.
- [2] Jarrah, M. A., "Low Speed Wind Tunnel Investigation of Flow about Delta Wings, Oscillating in Pitch to Very High Angle of Attack," AIAA Paper 89-0295, 1989.
- [3] Hanff, E. S., and Jenkins, S. B., "Large-Amplitude High-Rate Roll Experiments on a Delta and Double Delta Wing," AIAA Paper 90-0224, 1990.
- [4] Michael, C., and Francis, S., "X-31 Enhanced Fighter Maneuverability Demonstrator: Flight Test Achievements," International Council of the Aeronautical Sciences, Rept. 94-7.2.2, 1994.
- [5] Zhongjun, W., and Edward, C. L., "Unsteady Aerodynamic Effects on the Flight Characteristics of an F-16X1 Configuration," AIAA Paper 2000-3910, 2000.
- [6] Takagi, T., and Sugeno, M., "Fuzzy Identification of Systems and Its Applications to Modeling and Control," *IEEE Transactions on Systems, Man, and Cybernetics*, Vol. 15, No. 1, 1985, pp. 116–132.
- [7] Huang, D., and Wu, G., "Dynamic Derivative Simulation and Mathematical Model of the Wind Tunnel Test about a Model Pitching in Very Large Amplitude," *Acta Aerodynamica Sinica*, Vol. 17, No. 2, 1999, pp. 219–223.